Taiwania 63(3): 251-266, 2018
DOI: 10.6165/tai.2018.63.251

A dynamic downscaling approach to generate scale-free regional climate data in Taiwan

Huan-Yu LIN[1,2,3], Jer-Ming HU[1], Tze-Ying CHEN[3,4], Chang-Fu HSIEH[1,3], Guangyu WANG[5], Tongli WANG[5,6,*]

1. Institute of Ecology and Evolutionary Biology, National Taiwan University, 1 Roosevelt Rd., Section 4, Taipei 106, Taiwan.
2. Taiwan Forestry Research Institute, 53 Nanhai Rd., Taipei 100, Taiwan.
3. Biodiversity Association of Taiwan, 1 Shennong Rd., Section 1, Yilan City, Yilan County 260, Taiwan.
4. Department of Forestry and Natural Resources, National Ilan University, 1 Shennong Rd., Section 1, Yilan City, Yilan County 260, Taiwan.
5. Faculty of Forestry, University of British Columbia, Vancouver, BC, V6T 1Z4, Canada.
6. Department of Forest and Conservation Science, University of British Columbia, Vancouver, BC, V6T 1Z4, Canada.
[*]Corresponding author's e-mails: tongli.wang@ubc.ca

(Manuscript received 10 April 2018; accepted 17 July 2018; online published 10 August 2018)

ABSTRACT: Plenty of climate data from various sources have become available in recent years. However, to obtain climate data adequately meeting the requirement of ecological studies remains a challenge in some cases due to the difficulty of data integration and the complexity of downscaling, especially for mountainous regions. Lapse rate is one of the most important factors that influence the change of climatic variables in the mountains, and it should be incorporated into climatic models. In this study, we applied a synthetic approach combining bilinear interpolation (to produce seamless surfaces) and dynamic local regression (to obtain local lapse rates) to develop a scale-free and topography-correspondent downscaling model in R environment for Taiwan, called *clim.regression*. This model can generate 73 climatic variable estimates specific to the user-defined points of interest, including primary climatic variables and additional biologically relevant derivatives for historical (1960–2009) and future periods (2016–2035, 2046–2065 and 2081–2100). Results of our evaluation indicated that *clim.regression* reduced prediction error by 54.6%–66.7% relative to the original gridded climate data for temperatures. In addition, we demonstrated the spatiotemporal patterns of lapse rate for different climate variables.

KEY WORDS: Climate change, Downscaling model, Dynamic local regression, Historical and future climate scenarios, TCCIP.

INTRODUCTION

Climate variables, particularly temperature and precipitation, are the most well-known key factors related to vegetation zonation. A high-quality and accessible climate dataset is essential for ecological studies and applications, especially in regions with diverse topography and high climatic heterogeneity. However, to obtain and to process substantial climate data were difficult for ecologists in the past, and scientists often use statistically interpolated climate data from a few existing stations as substitutes for the continuous climate surface (Su, 1984a; Tang and Ohsawa, 1997).

Over the last decade, a large volume of climate data has become available through various sources; most of them were represented in grid format with the finest resolution of arc-seconds or kilometers in global or regional scale (Hannaway *et al.*, 2005; Hijmans *et al.*, 2005; Harris *et al.*, 2014). Although such gridded data are suitable for modeling general patterns and trends at global and regional scales, they are still too coarse to provide detailed climatic information in mountainous and topographically diverse areas to facilitate local ecological studies and resources management. To overcome this limitation, several downscaling methods have been developed to generate high-resolution spatial climate data, such as Ordinary Kriging (Chiu and Lin, 2004), a combination of Kriging and polynomial linear regression (Chiou *et al.*, 2004), a combination of bilinear interpolation and partial derivative functions for elevational adjustment (Wang *et al*., 2006; 2012), and an approach of dynamic local regression (Wang *et al.*, 2016; 2017). ClimateAP, a scale-free climate downscaling model based on dynamic local regression approach, was recently developed and covered Asia-Pacific (AP) region (Wang *et al.*, 2017). The baseline data of this model used a 4-km gridded climate data from PRISM (Daly *et al.* 2002) for China and Mongolia, and WorldClim (Hijmans *et al.* 2005) for the rest of the Asia-Pacific. The model reduces prediction error by up to 27% and 60% for monthly temperature and precipitation, respectively, relative to the original baseline data. However, the prediction accuracy for a specific region varies depending on the quality of the baseline data, which is affected by the density of weather stations used for developing the baseline data for the region. Unfortunately, historical climate data from weather stations in Taiwan were not included in the climate mapping project of PRISM (Hannaway *et al.*, 2005). Thus, it could adversely impact the prediction accuracy of ClimateAP in Taiwan.

Taiwan is a subtropical island on the west edge of the Pacific Ocean with diverse and complicated topography. The climate of Taiwan is mainly affected by the northeast monsoon during winter and by the southwest monsoon and typhoons in the summer. The Central Range occupying more than 70% of the area of Taiwan, runs through the whole island from northeast to southwest with the highest peak of 3,952 meters a.s.l., and creates an obvious altitudinal temperature zonation (Su, 1984a), as well as the seasonal allocation of precipitation (Su, 1985). Many studies have revealed a strong relationship between the natural vegetation and the large-scale altitudinal climate zonation (Su, 1984b; Chiu, 2004; Chiou *et al.*, 2010; Lin *et al.*, 2012; Li *et al.*, 2013). Furthermore, the local climate is induced by the co-effects of monsoon and topography (Sun, 1993; Sun *et al.*, 1998; Chao *et al.*, 2007; Chao *et al.*, 2010; Li *et al.*, 2013). Ecologists have a strong demand on fine-scale climate data to depict the ecological and environmental correlations in detail. However, most studies can only utilize indirect variables such as elevation and topography as substitutes to climatic variables due to the lack of a high-quality and high-resolution spatial climate dataset for the island.

Meteorologists in Taiwan have accomplished a framework called Taiwan Climate Change Projection and Information Platform (TCCIP) and generated a 5km×5km gridded climate surface based on historical observations from thousands of weather stations and provided future projections based on different AR5 General Circulation Models (GCMs) and scenarios (Hsu *et al.*, 2011; Weng and Yang, 2012). TCCIP's datasets are powerful supplements to the remote and observation-sparse mountains, but its resolution is not fine enough to represent the diverse climate situation due to the steep topography within a 5km×5km grid.

In this study, our main objectives were to: (1) establish a statistical downscaling model named as *clim.regression* in R environment to downscale the 5km×5km gridded climate data of TCCIP to a scale-free format based on the algorithm of bilinear interpolation and dynamic local regression from ClimateNA (Wang *et al.*, 2016) and ClimateAP (Wang *et al.*, 2017); (2) generate additional biologically relevant derivatives for ecological studies; (3) analyze the spatiotemporal patterns of variation in lapse rate; and (4) evaluate the prediction accuracy of *clim.regression* in comparison to the original TCCIP data.

MATERIALS AND METHODS

Source of historical and future climate data

The 5km×5km gridded surfaces of historical meteorological data used in this study were developed by TCCIP (Weng and Yang, 2012). The dataset covers the main island of Taiwan and spans the period from 1960 to 2009. TCCIP incorporated historical records of air temperature from 1,152 weather stations and precipitation from 1,497 rainfall stations to construct the gridded dataset through a conventional spatial interpolation process. There are four sets of primary climate variables including monthly precipitation (precip01 to precip12), monthly minimum temperature (Tmin01 to Tmin12), monthly mean temperature (Tmean01 to Tmean12) and monthly maximum temperature (Tmax01 to Tmax12). The values of these variables were obtained and united with the coordinate (latitude, longitude and elevation) of the center of each grid. There were 48 primary monthly climate variables in total. TCCIP has also provided future climate projections in the same resolution of 5km×5km, which were downscaled from GCMs of CMIP5 and rectified by observations of Aphrodite (Asia Precipitation Highly-Resolved Observational Data Integration Towards Evaluation of the Water Resources) and historical climate data of Taiwan (Lin *et al.* 2016). Projections of 49 GCMs (Table 1) covering different RCPs (RCP 2.5, RCP 4.6, RCP 6.0 and RCP 8.5) and periods (2016–2035, 2046–2065, 2081–2100).

The downscaling process of historical and future climate data

To obtain smooth and continuous climate surface estimates, *clim.regression* utilized the combination of bilinear interpolation and dynamic local regression approach to downscale the original 5km×5km gridded climate dataset to scale-free point estimates, which is the same as in ClimateNA (Wang *et al.* 2016) and ClimateAP (Wang *et al.* 2017). The downscaling process included four steps for each of the 48 primary monthly climate variables as illustrated in Figure 1:

(1). Extraction of a primary climate variable and elevation from the grid covering the point of interest and eight neighboring grids (Fig. 1A);
(2). Calculation of the bilinear interpolated estimate of the primary monthly climate variable (t'_p) and elevation (Z'_p) of the location of interest from the nearest four grids (Fig. 1B, Formula 1 & 2);
(3). Calculation of the differences in the primary monthly climate variable (Δt) and in elevation (Δz) between each of the 36 unique pairs among the nine neighbor grids (Fig. 1C, Formula 3);
(4). Construction of a simple linear regression based on the 36 pairs to represent the local relationship between Δt and Δz with the slope of the regression line, m, representing the local lapse rate of the cell where the interest point is located. Elevation adjustment was based on the lapse rate (m) and the difference between actual elevation (Z_p) and the bilinear interpolate (Z'_p) of the interest point (Fig. 1D, Formula 4).

Table 1. All the 49 GCMs and emission scenarios provided by TCCIP available for *clim.regression*.

GCM	RCP 2.6	RCP 4.5	RCP 6.0	RCP 8.5	GCM	RCP 2.6	RCP 4.5	RCP 6.0	RCP 8.5
10th-percentile	V	V	V	V	GFDL-ESM2M		V	V	V
25th-percentile	V	V	V	V	GISS-E2-H	V	V	V	V
75th-percentile	V	V	V	V	GISS-E2-H-CC		V		V
90th-percentile	V	V	V	V	GISS-E2-R	V	V	V	V
ACCESS1-0		V		V	GISS-E2-R-CC		V		V
ACCESS1-3		V		V	HadGEM2-AO	V	V	V	V
bcc-csm1-1	V	V	V	V	HadGEM2-CC		V		V
bcc-csm1-1-m	V	V	V	V	HadGEM2-ES	V	V	V	V
BNU-ESM	V	V		V	inmcm4		V		V
CanESM2	V	V		V	IPSL-CM5A-LR	V	V	V	V
CCSM4	V	V	V	V	IPSL-CM5A-MR	V	V	V	V
CESM1-BGC		V		V	IPSL-CM5B-LR		V		V
CESM1-CAM5	V	V	V	V	maximum	V	V	V	V
CESM1-CAM5-1-FV2		V		V	media	V	V	V	V
CMCC-CESM				V	minimum	V	V	V	V
CMCC-CM		V		V	MIROC5	V	V	V	V
CMCC-CMS		V		V	MIROC-ESM	V	V	V	V
CNRM-CM5	V	V		V	MIROC-ESM-CHEM	V	V	V	V
CSIRO-Mk3-6-0	V	V	V	V	MPI-ESM-LR	V	V		V
EC-EARTH				V	MPI-ESM-MR	V	V		V
ensemble	V	V	V	V	MRI-CGCM3	V	V	V	V
FGOALS-g2	V	V		V	MRI-ESM1				V
FIO-ESM	V	V	V	V	NorESM1-M	V	V	V	V
GFDL-CM3	V	V	V	V	NorESM1-ME	V	V	V	V
GFDL-ESM2G	V	V	V	V					

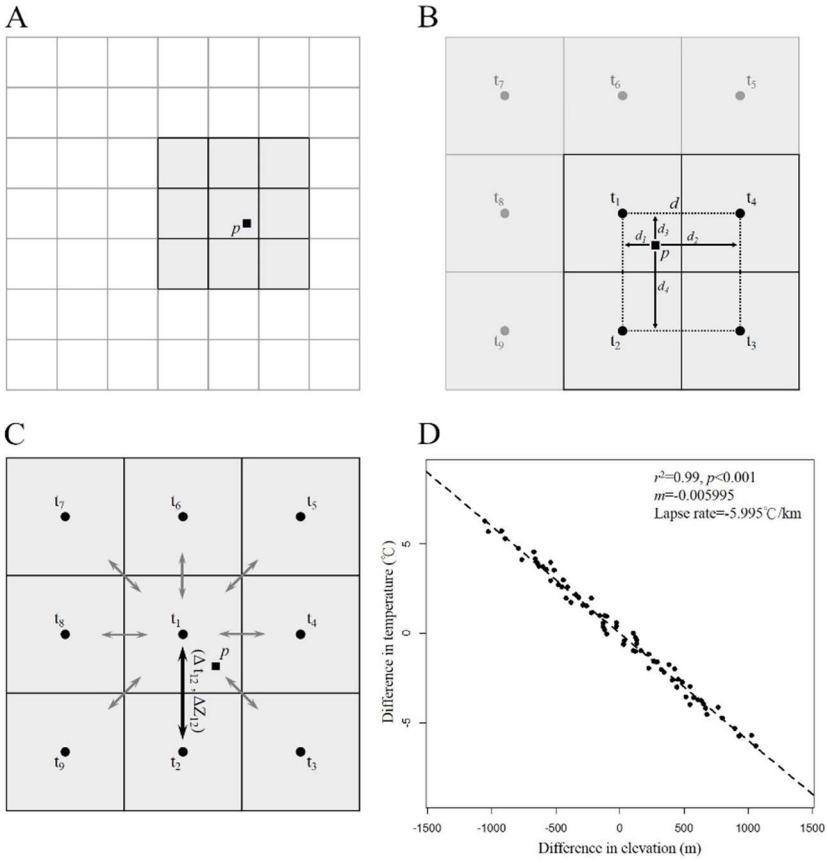

Fig. 1. Four steps of the downscaling process. (**A**) The grid tiles covering the point of interest *p* and its eight neighbors were extracted from the original climate dataset. (**B**) Bilinear interpolated estimates of temperature, precipitation and elevation of the point *p* were calculated by the weighting of distance to the center of the four nearest grid tiles. (**C**) A total of 36 unique pairs were subset to calculate the paired differences for temperature, precipitation (Δt) and elevation (Δz), respectively. (**D**) A simple linear regression of Δtmn~ΔZmn was conducted to obtain the slope *m*, representing the local lapse rate of the nine grids surround point of interest for each of the climate variables.

Clim.regression generated 73 climate variable estimates (Table 2) for either a single point location or a continuous surface. These climate variables were either directly calculated from the four primary climate variables or derived as indicated in Table 2.

The formula for the downscaling process included:

(1) $t_p^{'} = \frac{t_1 d_2 d_4 + t_2 d_2 d_3 + t_3 d_1 d_3 + t_4 d_1 d_4}{d^2}$

(2) $Z_p^{'} = \frac{Z_1 d_2 d_4 + Z_2 d_2 d_3 + Z_3 d_1 d_3 + Z_4 d_1 d_4}{d^2}$

(3) $\Delta t_{mn} \sim \Delta Z_{mn},\ m = \{1,2,3,\ldots,9\}, n = \{1,2,3,\ldots,9\},\ m \neq n$

(4) $t_p = t_p^{'} + m\left|Z_p - Z_p^{'}\right|$

Future climate projections of TCCIP were presented as anomalies relative to the baseline of 1986–2005 at the same spatial resolution of historical climate data. The anomalies of 5km×5km gridded future climate projections were added to the baseline portion (1986–2005) to create a 'gridded future climate data' prior to the downscaling procedure.

Table 2. Primary climate variables and the biologically relevant derivatives generated by *clim.regression*.

(1) Primary climate variable estimates.
(Category/Climate variables)
Precipitation
Monthly precipitation (precip01 to precip12)
Seasonal precipitation
(PPT_DJF, PPT_MAM, PPT_JJA, PPT_SON)
Mean annual precipitation (MAP)
Mean annual summer precipitation (MSP)
Temperature
Minimum
Mean monthly minimum temperature
(Tmin01 to Tmin12)
Mean seasonal minimum temperature
(Tmin_DJF, Tmin_MAM, Tmin_JJA, Tmin_SON)
Average
Mean monthly temperature (Tmean01 to Tmean12)
Mean seasonal temperature
(Tave_DJF, Tave_MAM, Tave_JJA, Tave_SON)
Mean annual temperature (MAT)
Maximum
Mean monthly maximum temperature
(Tmax01 to Tmax12)
Mean seasonal maximum temperature
(Tmax_DJF, Tmax_MAM, Tmax_JJA, Tmax_SON)
(2) Derivative estimates. (Derivative variable/Definition)
Temperature difference (TD): Tmean07 minus Tmean01
Summer heat:moisture index (SHM):
(Tmean07)/(MSP/1000)
Annual heat:moisture index (AHM): (MAT+10)/(MAP/1000)
Ratio of winter precipitation (WPR): PPT_DJF/MAP (Li *et al.*, 2013)
Warmth index (WI): Annual summation of mean monthly temperature higher than 5°C. (Su, 1984b)
Precipitation deficiency (PD): Difference between annual potential evapotranspiration and MAP. (Su, 1985)
Dry month (DM): The month with rainfall less than 2X mean monthly temperature. DM is a factor variable in 0/1. (Su, 1985)

Evaluations of climate variable estimates

We collected historical records covering the period of 1961 to 2009 from 15 weather stations to evaluate the accuracies of *clim.regression* model. Ten of the 15 stations are subordinate to the Central Weather Bureau (CWB), which is the main corporation agency of TCCIP. The remaining five stations belong to the Taiwan Forestry Research Institute (TFRI), which is independent of the samples of TCCIP network. The observations from the 15 weather stations were also used to evaluate the magnitude of improvement over the original TCCIP gridded surfaces. Four sets of climate variable estimates generated by *clim.regression*, including monthly precipitation, monthly minimum temperature, monthly mean temperature and monthly maximum temperature, were evaluated against observations from the 15 weather stations (Table 3, Fig. 2). Prediction errors of *clim.regression* were assessed and compared using the following three statistical measures:

Mean error (ME):

$\frac{1}{n}\sum(y_i - f_i)$

, where n is the number of samples, fi is the predicted value of the i-th sample and yi its real value.

Mean absolute error (MAE):

$\frac{1}{n}\sum|y_i - f_i|$

Root mean squared error (RMSE):

$\sqrt{\frac{1}{n}\sum(y_i - f_i)^2}$

Table 3. Localities of 15 weather stations and the period of observed data that available for model evaluation.

Subordination/ Station	Longitude	Latitude	Altitude (m)	Observation period
Central Weather Bureau (CWB) Incorporated by TCCIP				
Kaohsiung	120.32	22.57	2	1961–2009
Taitung	121.15	22.75	9	
Hualien	121.61	23.98	16	
Hengchun	120.75	22.00	22	
Keelung	121.74	25.13	27	
Taichung	120.68	24.15	84	
Anbu	121.53	25.18	826	
Sunmoon Lake	120.91	23.88	1018	
Alishan	120.81	23.51	2413	
Yushan	120.96	23.49	3845	
Taiwan Forestry Research Institute (TFRI) independent from TCCIP				
Taimali	120.98	22.60	120	1980–2009
Liukuei	120.63	23.00	230	1999–2009
Fushan	121.60	24.76	634	1992–2003
Lienhuachih	120.90	23.93	666	1999–2009
Piluhsi	121.31	24.23	2150	1991–2009

Fig. 2. Long-term observation data from fifteen weather stations were incorporated to evaluate the downscaling model. Solid stars demonstrate stations subordinate to the Central Weather Bureau of Taiwan (CWB). Open stars represent stations belonging to the Taiwan Forestry Research Institute (TFRI), which were independent from TCCIP system.

Table 4. The R-square values of the local linear regressions for different monthly climate variables.

Monthly variable	R^2 value / Month												
	1	2	3	4	5	6	7	8	9	10	11	12	Average
Tmean	0.82	0.82	0.81	0.84	0.86	0.87	0.88	0.88	0.88	0.87	0.86	0.84	0.85
Tmin	0.79	0.80	0.81	0.83	0.85	0.85	0.85	0.85	0.86	0.84	0.83	0.80	0.83
Tmax	0.79	0.79	0.78	0.81	0.84	0.85	0.85	0.86	0.85	0.82	0.81	0.79	0.82
Precipitation	0.20	0.21	0.24	0.23	0.25	0.26	0.23	0.25	0.22	0.21	0.22	0.22	0.23

RESULTS

Scale-free climate surfaces from the downscaling model

Clim.regression is a scale-free and topography-correspondent downscaling model, which attributes to the continuous and smooth characteristics of bilinear interpolation and the elevational adjustment by lapse rate from a dynamic local regression. Regular grids for MAT (mean annual temperature) and MAP (mean annual precipitation) surfaces were generated by the model at the spatial resolution of the original baseline data (5km×5km) and a downscaled spatial resolution (250m×250m) (Fig. 3). The results showed that MAT in Taiwan ranges from 1 °C to 28 °C and exhibits a trend of decline from lowland to alpine and from south to north. A more detailed spatial distribution of temperature due to geographical effect, such as warm basin of Puli and cool tablelands of Linkou and Pagua, could also be revealed by the downscaled surface (Fig. 3A–B). The spatial distribution of MAP demonstrated a different pattern from that of MAT; it exhibited two-ended humid regions in the northeast and the southwest of Taiwan. The northeastern mountains in Taipei and Ilan and the southwestern edge of the Central Mountain Range in Kaohsiung and Pingtung are the moistest regions of Taiwan, and the downscaled surface more clearly revealed some precipitation hotspots with annual rainfall up to 6,000 mm (Fig. 3C–D).

In comparison with the original climate dataset at the resolution of 5km×5km, the downscaled one offers a detail depiction on the climatic alternation with topographies as the examples showed in Fig. 3. The scale-free modeling approach not only has the advantage in providing continuous and seamless climatic surface for large-scale studies (e.g., the classification of ecological-climatic regions, climatic niche modeling, and projections, etc.), but also generates accurate and point-specific climatic estimates as environmental correlates for plot-based researches (e.g., vegetation survey and plotting, etc.).

Lapse rate and effectiveness of the elevational adjustment

The dynamic local linear regression among the nine neighboring cells explained, on average, 85.3% of the total variation in monthly mean temperature. The amount of variance explained for monthly minimum temperature (83.1%) and monthly maximum temperature (81.9%) were slightly lower (Table 4). The average temperature lapse rate in the mountain areas was -5.65 °C/km but displayed an obvious seasonal variation. Fig. 4A–C illustrate the same pattern in three primary temperature variables with a higher variation of lapse rate in winter (from Nov. to Apr.) than in summer (from May to Sep.). The relationships revealed in the local regressions were weaker for precipitation than for temperatures. Only 20.3–25.7% of precipitation's variation can be explained by the local regressions (Fig. 4D, Table 4).

We compared the relationships between the changes in temperature and the elevation between two mountains, Alishan and Taipingshan. Such a relationship was stronger for Alishan with a steady lapse rate from -6.00 to -6.44 °C/km from winter to summer. In contrast, a higher seasonal variation and a weaker relationship between temperature and elevation were observed in Taipingshan (Fig. 5).

The spatial distributions of the estimated lapse rates varied among seasons and regions. In winter, lower lapse rates for monthly average temperature (from -2 to -5 °C/km) were exhibited in the central and western parts of the Central Mountain Range, especially in the hills from Hsinchu, Miaoli, Nantou, Chiayi to Kaohsiung. In contrast, very steep lapse rates (from -6 to -9 °C/km) were demonstrated in the northeastern mountains and Hengchun peninsula (Fig. 6A). The spatial differentiation in lapse rate in most areas mitigated in summer, and demonstrated a mild geographical divergence with a range from -4 to -7 °C/km (Fig. 6C). In some regions, such as the northeastern mountains in Taipei and Ilan, Hengchun peninsula, Tawu Mountain and the Costal Mountain Range, the steep lapse rates (<-6 °C/km) could be found across all seasons of the year. Our dynamic local regression approach revealed the variation in the lapse rate both spatially and temporally over the island, and thus produced accurate adjustment for elevation.

Statistical evaluations of the downscaling model and its improvement over TCCIP dataset

The prediction accuracy of *clim.regression* was evaluated by comparing to historical observations from the 15 weather stations (Table 5). *Clim.regression* demonstrated a high prediction accuracy for monthly mean temperature with a low prediction error (0.56 °C in MAE) and a high percent of variance explained (99.1%). The prediction accuracy and variance explanation were slightly lower for monthly minimum temperature and

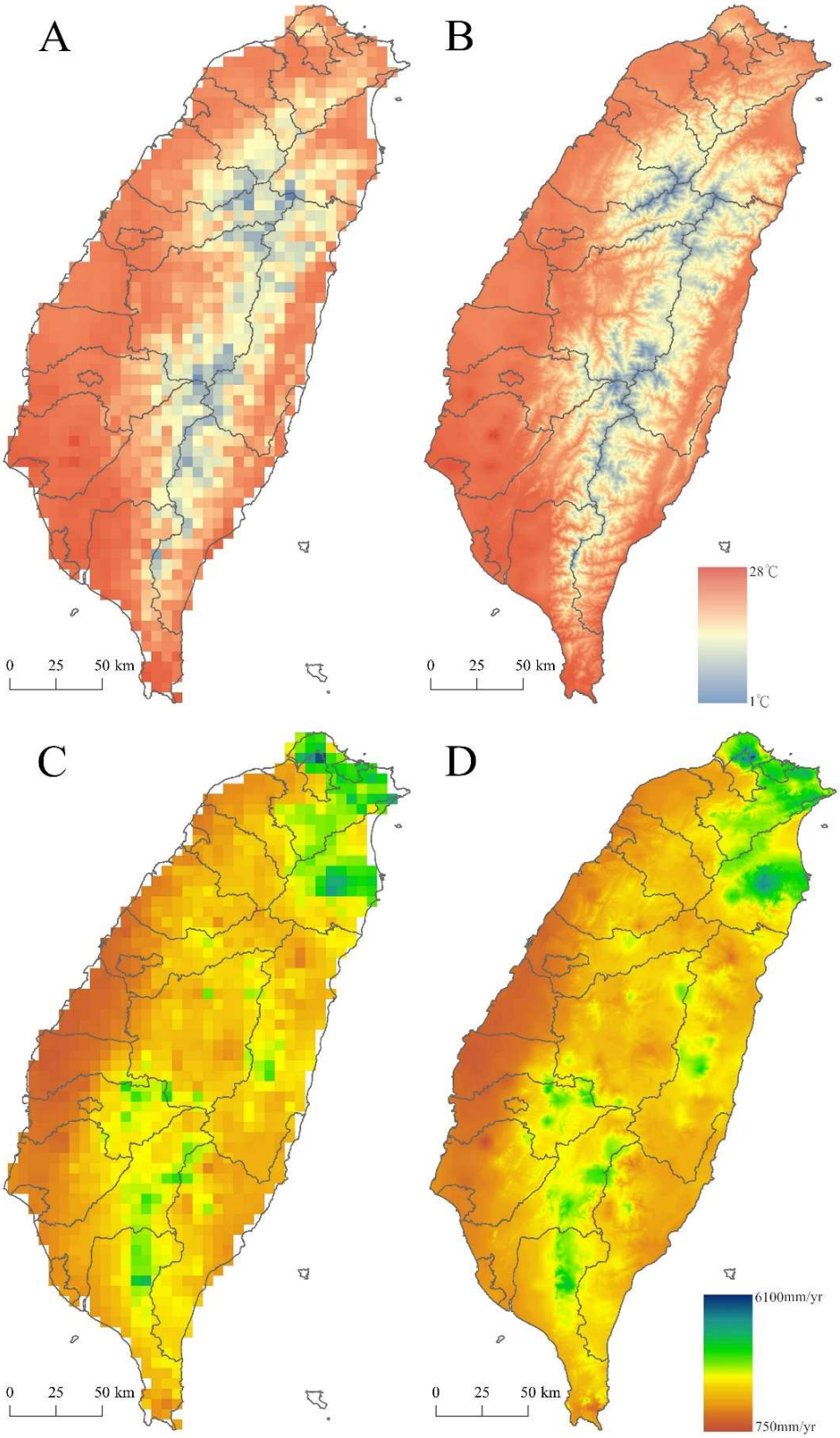

Fig. 3. Spatial distributions of mean annual temperature (MAT) and mean annual precipitation (MAP) for original climate data at the resolution of 5 km and downscaled to the resolution of 250 m. (**A**) Original and (**B**) downscaled MAT; (**C**) Original (**D**) and downscaled MAP. Data period: 1986–2005.

Table 5. Summaries of statistical evaluations of *clim.regression* against historical observed data from Central Weather Bureau (CWB) and Taiwan Forestry Research Institute (TFRI).

Subordination	Climate variable	*Clim.regression*			TCCIP		
		MAE	RMSE	Variance explained (%)	MAE	RMSE	Variance explained (%)
CWB (10 stations)	Tmean (℃)	0.56	0.73	99.10	1.73	3.40	87.83
	Tmin (℃)	0.79	0.98	98.72	1.92	3.51	87.04
	Tmax (℃)	0.71	1.00	98.22	1.67	3.25	88.29
	Precipitation (mm)	34.65	64.63	94.39	31.10	67.08	93.75
TFRI (5 stations)	Tmean (℃)	0.58	0.74	98.56	1.34	1.56	96.75
	Tmin (℃)	0.82	1.17	97.27	1.24	1.49	96.51
	Tmax (℃)	1.52	1.85	95.61	2.53	2.78	92.27
	Precipitation (mm)	49.56	105.39	79.77	46.39	106.14	79.62
Average (15 stations)	Tmean (℃)	0.56	0.73	99.06	1.68	3.25	86.71
	Tmin (℃)	0.79	1.00	98.52	1.85	3.35	86.61
	Tmax (℃)	0.80	1.13	97.61	1.76	3.21	84.76
	Precipitation (mm)	36.26	70.16	93.00	32.74	72.30	92.43

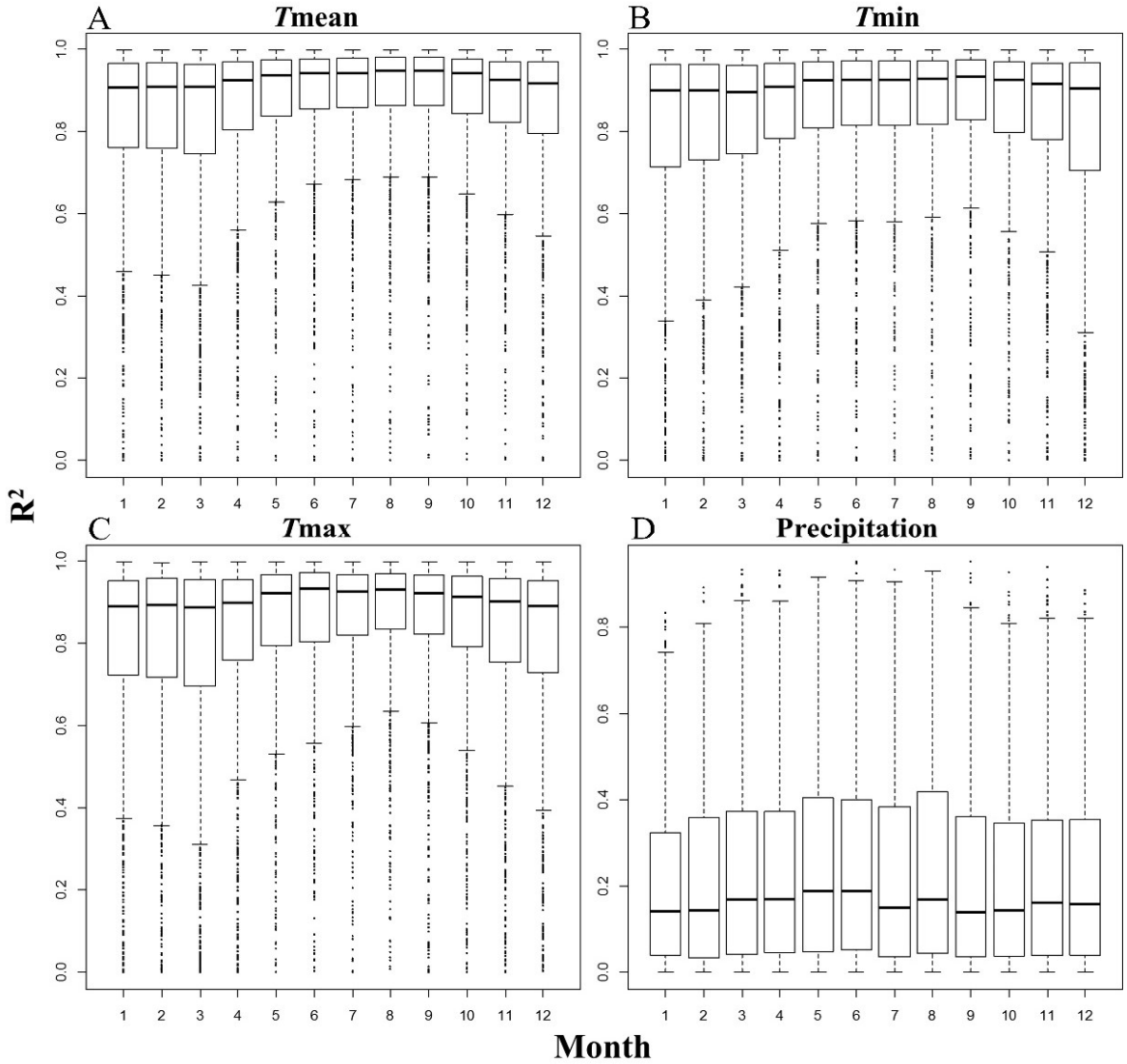

Fig. 4. Proportions of variance explained by local linear regressions in total variation among the nine neighboring cells for the four primary climate variables: (**A**) monthly mean temperature (Tmean), (**B**) monthly minimum temperature (Tmin), (**C**) monthly maximum temperature (Tmax) and (**D**) monthly precipitation, by month. The black horizontal solid lines inside the boxes indicate the medium. For temperature variables, a similar trend of higher variation in winter and lower variation in summer can be observed. Data period: 1961–2009.

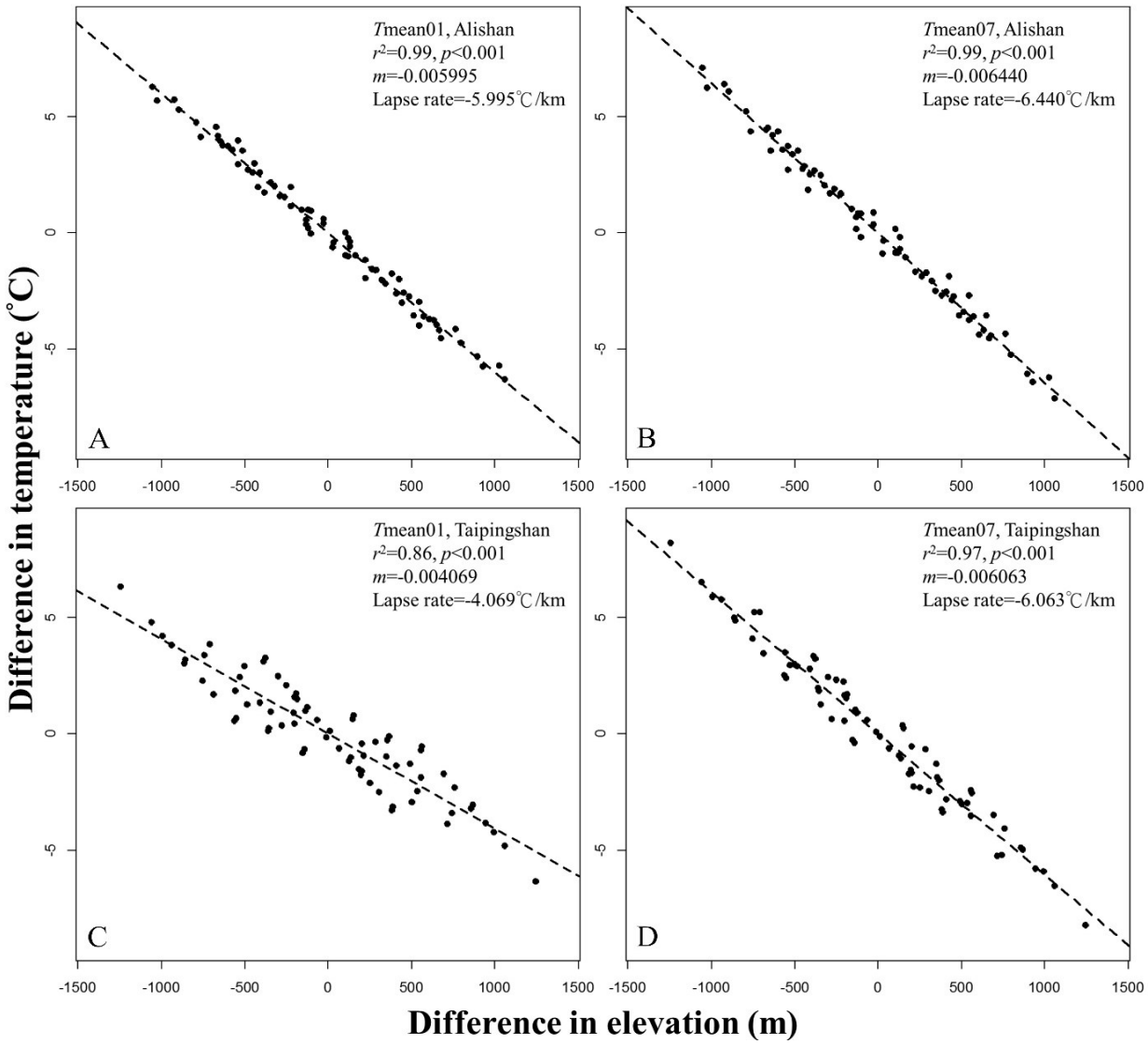

Fig. 5. Comparisons in lapse rates for winter and summer between two mountains, Alishan (**A**, **B**) and Taipingshan (**C**, **D**). Alishan (120.81E, 23.51N) is a mountain located in the south-west Taiwan, while Taipingshan (121.53E, 24.49N) is located in the north-east part. The two mountains have a similar elevation around 2000 m. Data period: 1961–2009.

monthly maximum temperature in terms of the prediction error (0.79 °C and 0.80 °C) and the percent of variance explained (98.5% and 97.6%, respectively). However, the prediction accuracy was considerably lower for precipitation. The precipitation estimates explained 93.0% of the total variance of observations with a prediction error of 36.26 mm in MAE.

Monthly mean temperature was the most predictable climate variable. The prediction accuracy of monthly mean temperature in regions lower than 2,500 m a.s.l. could reach the level of 0.3–0.6 °C in MAE. However, we found that the prediction error increased with elevation (r^2=0.55, p=0.0015). For example, in the subalpine area of Taiwan, *clim.regression* had a comparatively weak predict ability with the MAE of 1.02 °C. Interestingly, such a relationship was not observed for monthly minimum temperature and monthly maximum temperature (r^2=0.07 and 0.35, p=0.3252 and 0.0209). The prediction accuracy for precipitation was lower and accompanied with a higher variation and a less amount of variance explained (92.1%). In addition, there was no obvious trend found between prediction error in precipitation and altitude (r^2=0.01, p=0.7612). It suggests that the pattern of precipitation could be dominantly influenced by regional terrains rather than a local elevational gradient within the 5km×5km grids.

In comparisons to TCCIP original dataset, *clim.regression* reduced prediction errors by 1.12°C (66.7%), 1.06°C (52.3%) and 0.96 °C (54.6%) for Tmean, Tmin and Tmax, respectively (Fig. 7A–C, Table 5). These results demonstrated that *clim.regression*

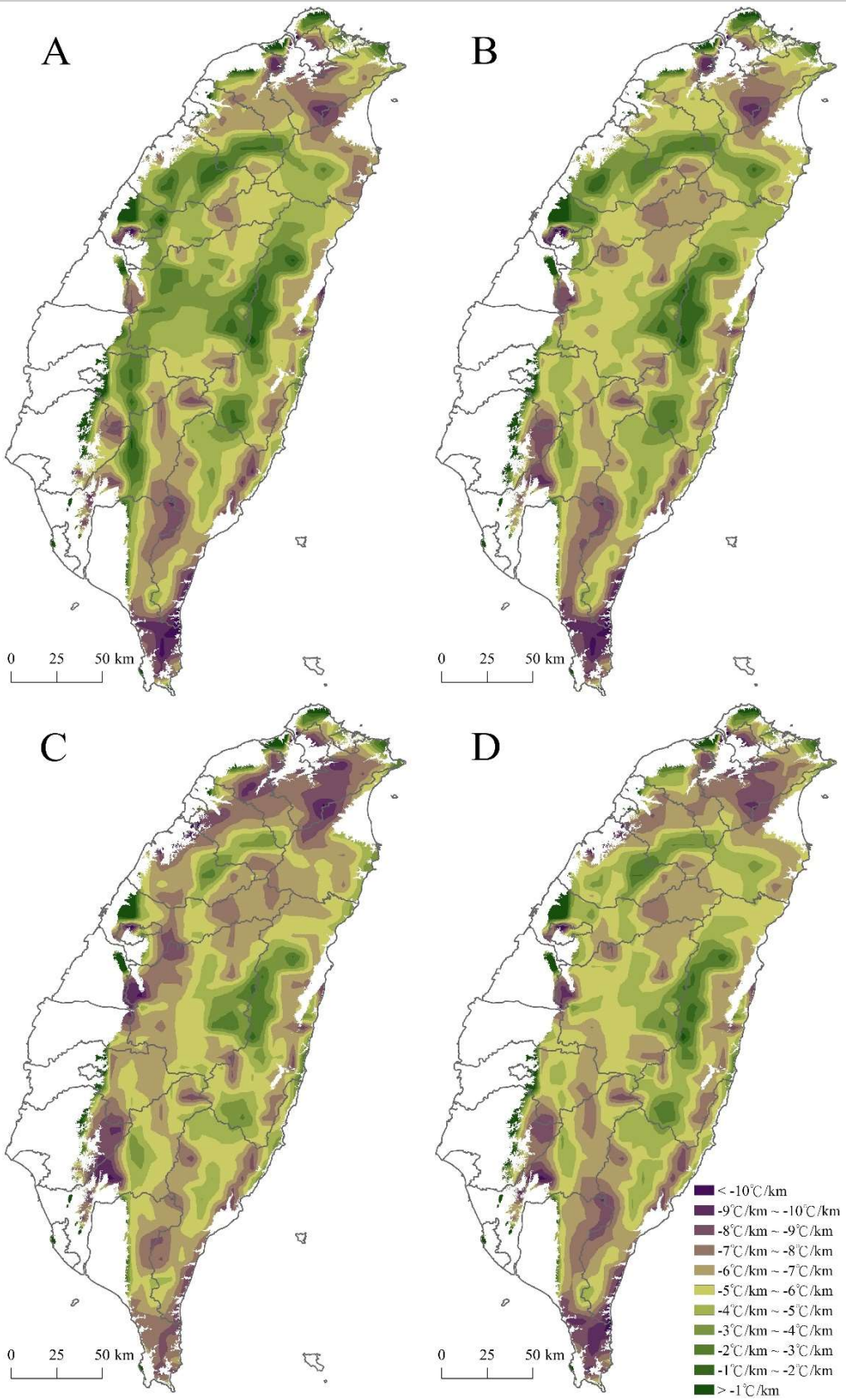

Fig. 6. Spatial distributions of estimated lapse rate for monthly mean temperature in the mountain areas (regions higher than 100 m a.s.l.) in Taiwan: (**A**) January, (**B**) April, (**C**) July and (**D**) October. Data period: 1961–2009; resolution: 250 m.

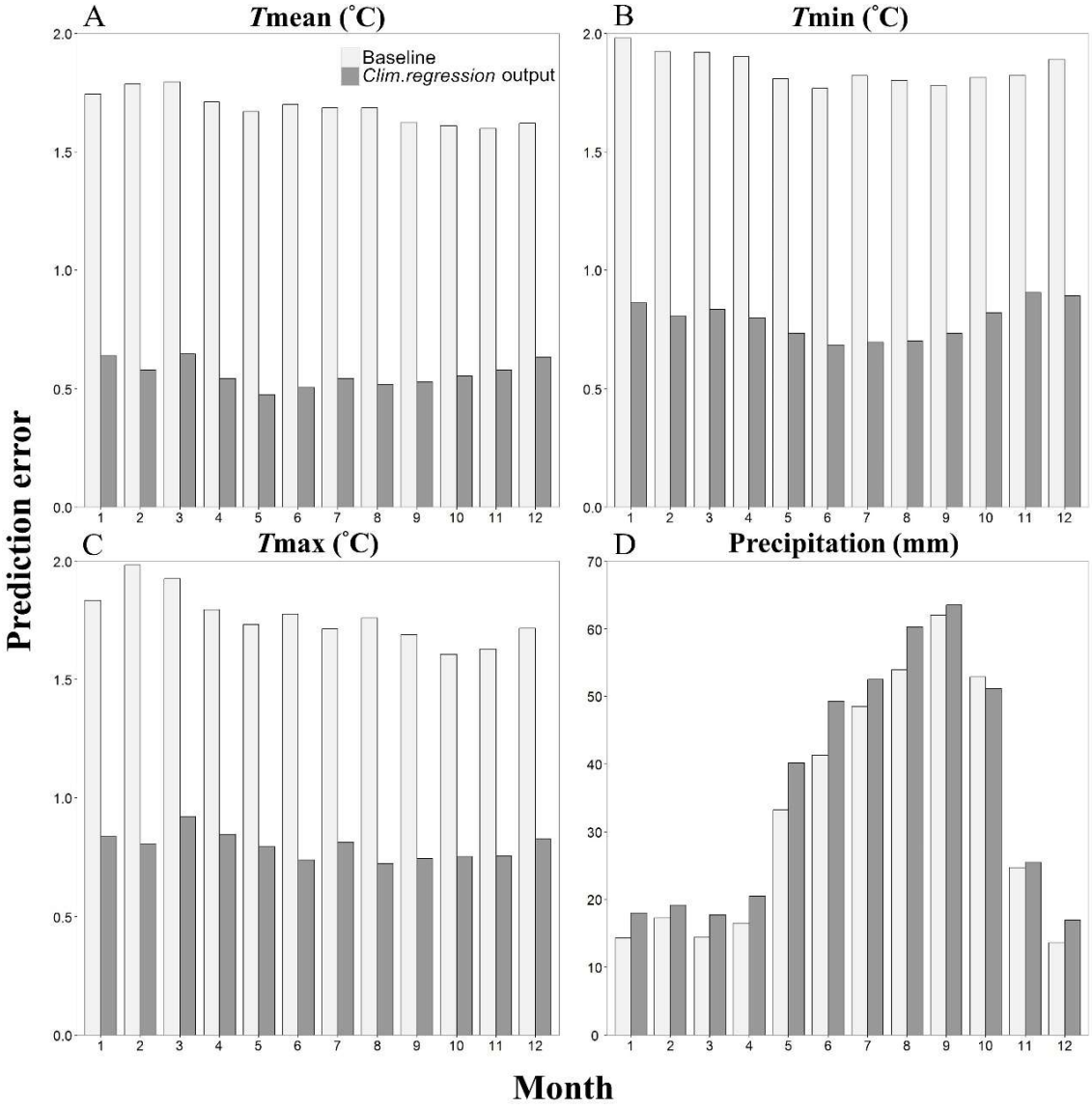

Fig. 7. Comparison in prediction error between baseline data (directly from TCCIP) and *Clim.regression* output of 15 weather stations for: (**A**) monthly mean temperature (Tmean), (**B**) monthly minimum temperature (Tmin), (**C**) monthly maximum temperature (Tmax) and (**D**) monthly precipitation.

effectively improved the accuracy and refined the spatial resolution of temperature estimates relative to the original dataset from TCCIP, especially with advantages in temperature projection for mountains with diverse topography. However, the improvement in precipitation is limited (Fig. 7D). Both TCCIP baseline and *clim.regression* had a higher prediction error for precipitation during summer months (May to Oct.). As illustrated in Fig. 8, the magnitude of the improvement was more substantial at higher elevations (the lower end of the temperatures), especially in the alpine area of Yushan (3,952m) and Alishan (2,413m). The downscaled temperatures followed a 1:1 relationship with observations much closer than the TCCIP predictions.

Downscaling for future climate projections

Based on the estimated lapse rate of future scenarios, *clim.regression* was also effective to downscale the 'gridded future climate data' to a scale-free and continuous surface with the same 73 climate variables as for the historical period. Downscaled MAT by *clim.regression* for the reference period and future scenario in the mountainous area of Taiwan were illustrated in Fig.9. The benefit of the downscaled MAT is clearly shown in this example in term of fine spatial resolution and high topographical correspondence. Based on the comparison among current and future climate under the RCP 4.5 scenario, not only an evident warming can be found in the valleys and plains but also demonstrate an obvious retreat of isothermals to the

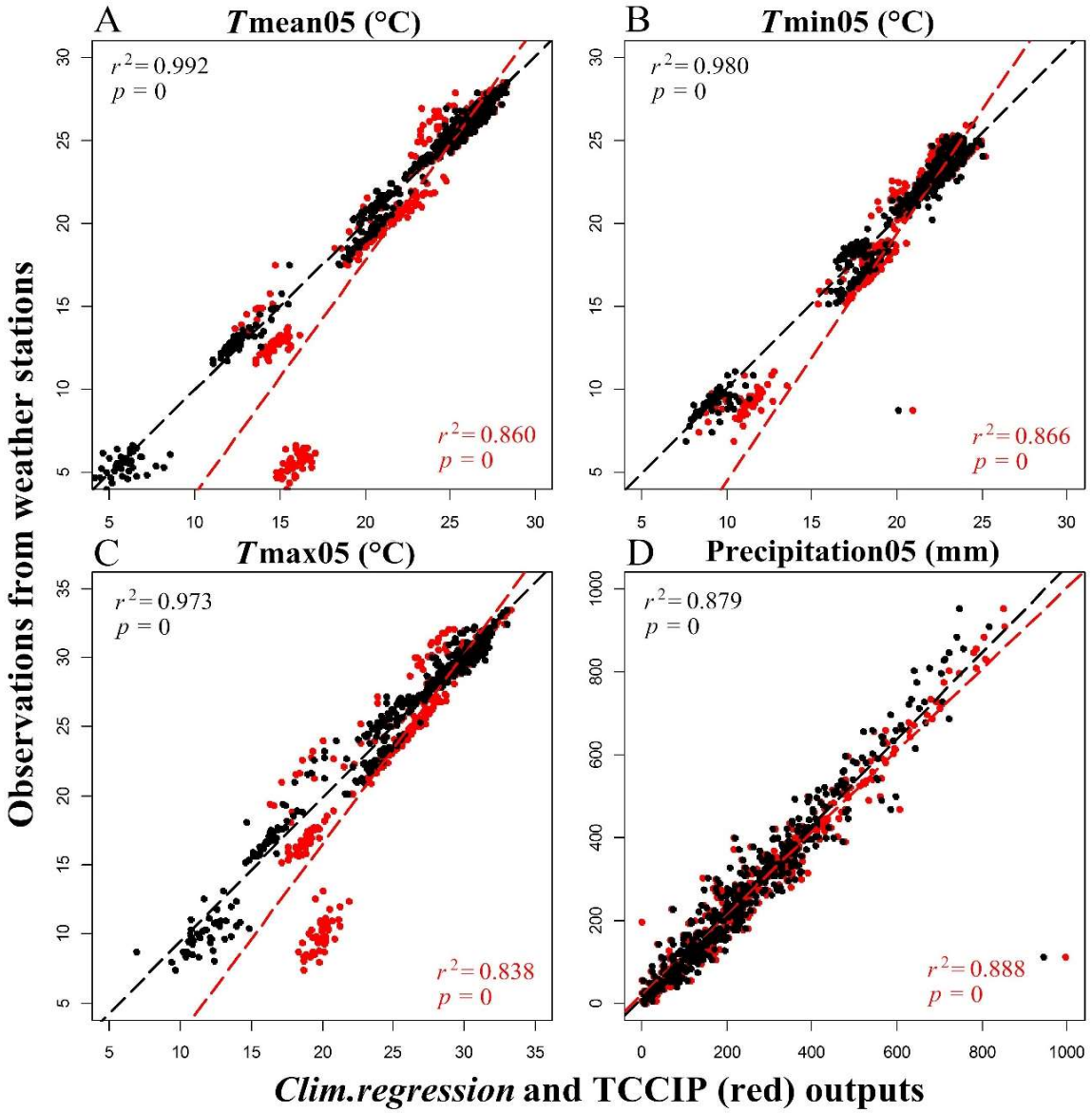

Fig. 8. An illustration to demonstrate the difference between observations from 15 weather stations and its corresponding climatic estimates from TCCIP outputs (red) and *clim.regression* in May for (**A**) monthly mean temperature (Tmean05), (**B**) monthly minimum temperature (Tmin05), (**C**) monthly maximum temperature (Tmax05) and (**D**) monthly precipitation (Precipitation05). It was clearly revealed that TCCIP outputs are biased as the decreasing of observed temperature, which is highly correspond to the raise of altitude.

subalpine area (Fig.9). *Clim.regression* has a solid advantage in generating current and future climate data with the same and desirable spatial resolution, which is a convenient for modeling biological response to climate change and for advanced comparative studies.

DISCUSSION

Spatio-temporal heterogeneity of temperature lapse rate in Taiwan

Temperature lapse rate, the rate of change in temperature with elevation in the troposphere, is widely used as the most important predictor in mountain climate (Su, 1984a; Tang, 2006; Chiu *et al.*, 2014). Many authors have revealed the spatio-temporal variation of lapse rate caused by atmospheric processes, interaction of prevailing monsoon, geographical and topographical positions, etc. (Su, 1984a; Tang and Ohsawa, 1997; Pepin, 2001; Chiu *et al.*, 2014), thus suggested using regional observed data to derive the lapse rate as a local climate predictor rather than the commonly used global constant (-6.5 °C/km in Barry and Chorely, 2009; or -6.0 °C/km in Willmott and Matsuura, 2009). In Taiwan, a high spatio-temporal variation of lapse rate has been reported. Su (1984a) mentioned that temperature in the mountain area is highly correlated to elevations, and

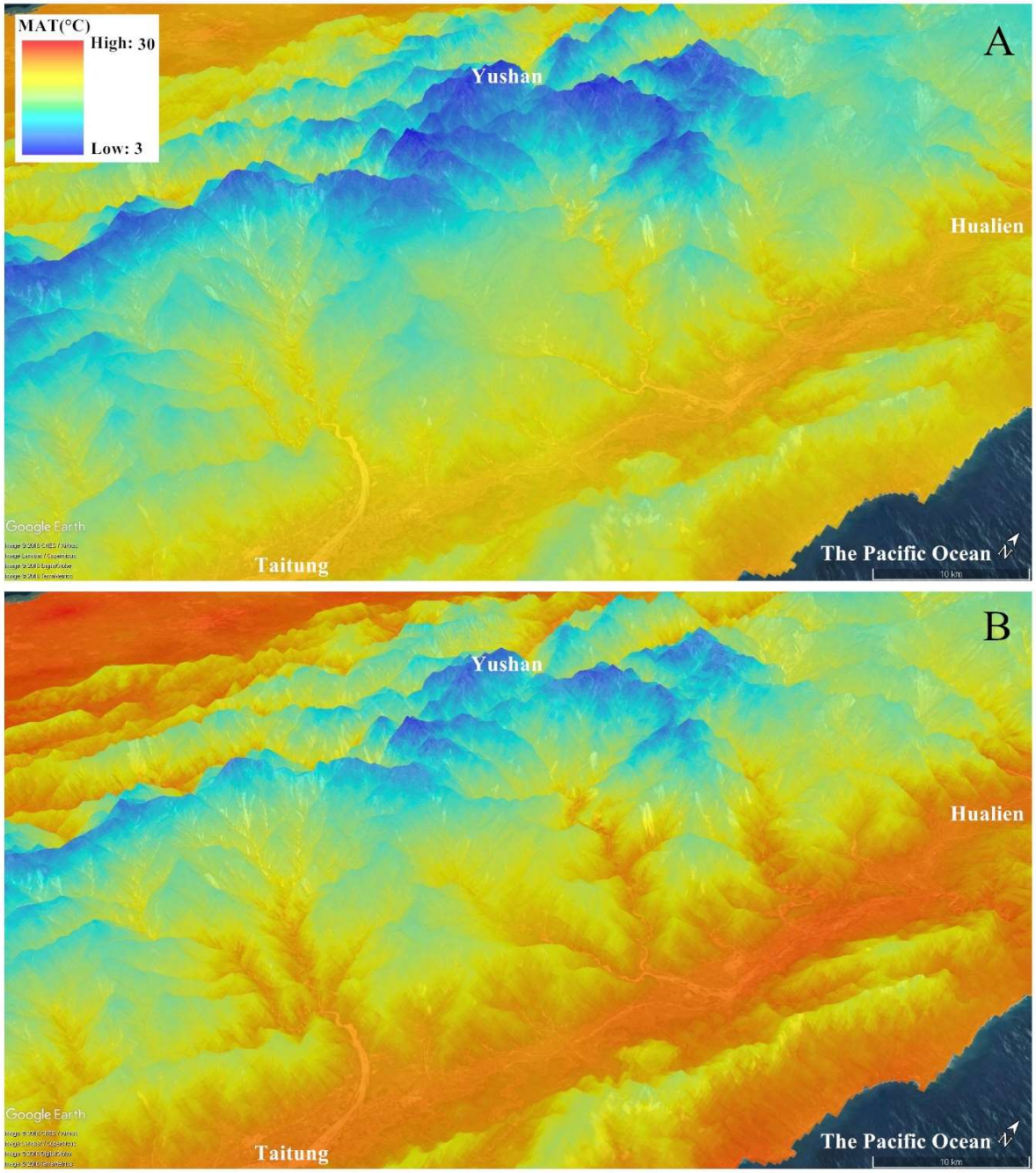

Fig. 9. Illustration of the effectiveness of downscaled climatic surface in the mountainous area of Taiwan, stretching from the coast of the Pacific Ocean up to the highest peak, Yushan, at 3,952 m a.s.l. (**A**) Downscaled mean annual temperature (MAT) by *clim.regression* in the resolution of 250 m for the reference period of 1986–2005; (**B**) downscaled future MAT for the period of 2090–2100 based on the GCM of CSIRO-Mk3-6-0 in RCP 4.5 scenario.

represented a lapse rate ranges from -3.08 to -6.98 °C/km but varies among regions and seasons. Guan *et al.* (2009) has modeled a steeper temperature lapse rate from April to December with a range between -4.93 and -5.62 °C/km, and a shallower rate from -3.22 to -3.61 °C/km during January to March according to historical observation data from 43 meteorological stations, mostly located in the west of the Central Mountain Range and Snow Mountain. A full exploration of the spatio-temporal variation of lapse rate was accomplished by Chiu *et al.* (2014). Based on historical records from 219 weather stations, Chiu *et al.* (2014) depicted that the average temperature lapse rate for all of Taiwan is -5.17 °C/km with a general tendency to be steeper in summer and shallower in winter. They also found that the lapse rate exhibits a pronounced contrast between the

windward side (steeper, -5.97 °C/km) and the leeward side of the Central Mountain Range (shallower, -4.51 °C/km) due to the atmospheric effect of prevailing winter monsoon. However, to obtain a lapse rate for specific locations remained a challenge.

Through the approach of dynamic local regression, we have delineated a fine scale of lapse rate and used it as the key adjustment for the downscaling procedure. The distribution maps of lapse rate for the monthly temperature (Fig. 6) have shown a similar spatio-temporal pattern to that of Chiu *et al.* (2014), which exhibited a steeper lapse rate in regions exposed to the northeast monsoon (e.g., The northeast mountains, the Coastal Mountain Range from Hualien to Taitung, and Hengchun peninsula) and shallower in the leeward side (e.g., The west of the Central Mountain Range) during winter, and became obscure in summer. In the context of high spatio-temporal variation of lapse rate in Taiwan, *clim.regression* shows an excellent performance by using the local lapse rate to facilitate a high-resolution downscaling. Our evaluations have proved that this model considerably improves prediction accuracy relative to the original TCCIP climate data and it is suitable for the steep and mountainous areas and provides accurate and topography-corresponded climate variable estimates.

In addition, Lenoir *et al.* (2008) have pointed out that temperature lapse rate is the most important predictor of temperature variability in mountains, and can be one of the key contributions to predict the response of plants to climate change. In this study, steep lapse rates (<-6 °C/km) are found all year round in several areas, such as the northeast mountains, Hengchun peninsula, Tawu Mountain and Coastal Mountain Range. Some studies have reported the compression of vegetation zones in these areas due to a dramatic change in temperature along the altitudinal gradient (Su 1984a; Su, 1984b; Chiou *et al.*, 2010). In consequence of the feature of local regression, *clim.regression* can provide a deep insight into the entire spatial and temporal distribution of lapse rate in Taiwan, and our results show a great promise for providing high quality scale-free climate variables for a wide spectrum of research and application activities in biology, ecology, and adaptation to climate change.

Benefits of the dynamic local downscaling model

Dynamic local regression is a simple but effective method to achieve a scale-free downscaling. This method has been utilized to develop ClimateNA for North America (Wang *et al.*, 2016) and ClimateAP for Asia-Pacific region (Wang *et al.*, 2017) to downscale WorldClim and PRISM gridded datasets to scale-free climate estimates. The model evaluation demonstrated that the prediction error of ClimateNA and ClimateAP are 0.77 °C and 1 °C (in MAE). *Clim.regression* is a R script based on the same algorithm of ClimateNA and ClimateAP but use TCCIP 5km×5km gridded climate surface, an interpolation based on historical data from thousands of weather stations of Taiwan, as the data source. Our statistical evaluations revealed that the prediction error of *clim.regression* is 0.56 °C in monthly mean temperature and 36.26 mm in monthly precipitation, which are substantially smaller than that for the original TCCIP data (in MAE, Table 5). These results suggest that the dynamic local regression approach is effective in downscaling climate variables to meet the requirement for ecological studies in mountain areas in Taiwan.

Chiu and Lin (2004) utilized regression and Ordinary Kriging to develop a scale-free model based on 219 meteorological stations and 877 rainfall stations to interpolate the distribution of monthly temperature and monthly precipitation. A cross validation revealed that the prediction errors of monthly temperature ranged from 1.57–1.74 °C and monthly precipitation ranged from 17.51–53.07 mm (in RMSE). In addition, some authors applied polynomial regression to model the distribution of monthly temperature based on historical observations from 156 weather stations, but exhibited a lower prediction accuracy ranging from -5.15 °C to 4.68 °C (in ME) due to the inflexibility of universal regression coefficient (Chiou *et al.*, 2004). In contrast, *clim.regression* provides more accurate temperature estimates (0.73–1.13 °C in RMSE) than using Kriging and polynomial regression, due to its flexibility of local lapse rate and the effectiveness of elevational adjustment. However the rainfall prediction error of our model is 70.16 mm in RMSE, it does not meet the level shown in Chiu and Lin (2004).

We found that *clim.regression* is not effective in downscaling precipitation (Fig. 7D). In Taiwan, the co-effect of humid monsoons and strong typhoons with diverse topography creates dramatic changes of precipitation in the mountains. For a windward slope at the middle elevation, the monthly precipitation during wet seasons can reach 2,000 mm/month but decrease to less than 800 mm/month as the change of aspect in a short distance of kilometers at the same elevation. Bilinear interpolation with a sampling window of 2 by 2 cells (10km×10km) and the dynamic local regression within a sampling unit of 3 by 3 cells (15km×15km) are the kernel of c*lim.regression* to produce climatic estimates for the point of interest, however, the severe change of precipitation in mountains may neither linearly correlate with the change of elevation nor correspondently fit with the coverage of sampling windows to lead to a poor performance in precipitation prediction than temperature. It is worthy of advanced researches to explore the spatial pattern and its statistical correlates of precipitation to achieve an accurate predict model in the future.

The results of validation by weather stations of CWB

and TFRI demonstrated that the estimates of *clim.regression* were more approximate to observations from CWB rather than TFRI. It could be partly attributed to the reason that most historical observation data of CWB stations were the main component of TCCIP system, so that it might not be an independent validation and could lead to an over estimation of both TCCIP and *clim.regression* model performances, but it would not affect the evaluation of the improvement in prediction accuracy relative to TCCIP. Historical observation data from TFRI was not included by TCCIP, so that an independent validation could be achieved theoretically. However, due to the lack of sustainable maintenance and long-term financial support, data quality of these independent weather stations could be harsher than CWB. It could be another effect leading to an under estimation of the downscaling model.

CONCLUSION

Ecologists have accumulated a large amount of field investigation data in Taiwan. Many studies exploring vegetation-climate relationship have also been published. However, due to the difficulty in accessing climate data in the past, researchers usually used geographical variables, such as elevation, longitude, latitude, aspect, the distance to seashore and exposure to prevailing monsoon as substitutions for climate variables in data analysis. Results of these studies based on indirect variables could lead to a biased result of ecological-climate relationships. The scale-free climate variables generated by *clim.regression* offer a solution to this problem. Users cannot only generate a continuous and seamless surface for climate niche modeling but is also possible to estimate historical and future climate condition for specific locations such as numerous vegetation survey plots. It provides a large number of climate variables for scientists to explore, delineate and quantify the relationships between climate and vegetation.

However, some limitations still exist in our downscaling approach. *Clim.regression* downscales gridded source climate variables through a combination of bilinear interpolation and concise elevational adjustment. Therefore, the performance of *clim.regression* is mostly determined by two factors in addition to the effectiveness of the downscaling algorithm: the quality of the original climate dataset and the accuracy of the imported digital elevation surface. The quality of baseline data strongly depends on the number of historical observations and the number of weather stations being incorporated. Therefore, we regard both of the robust meteorological observation network and the effective interpolation approaches are the critical issues to provide a high-quality gridded dataset for downscaling. TCCIP has an ongoing project to improve the accuracy and the coverage of periods for gridded climate data of Taiwan, which serves as an ideal baseline data to be used in *clim.regression* to generate high-resolution and high-quality climate data for ecological studies for ecosystem adaptation to climate change.

ACKNOWLEDGEMENTS

This study was supported by research grant "A study on the resilience of biodiversity under long-term climate change" (106AS-11.7.1-FB-e1) funded by Taiwan Forestry Bureau and "Adaptation of Asia-Pacific Forests to Climate Change Phase II" funded by the Asia-Pacific Network for Sustainable Forest Management and Rehabilitation and the University of British Columbia, Canada. The authors are also thankful to Taiwan Climate Change Projection and Information Platform for data providing.

LITERATURE CITED

Barry, R.G. and R.J. Choreley. 2009. Atmosphere, Weather and Climate, 9th edition, Routledge, London, 536 pp.

Chao, W.C., G.-Z.M. Song, K.J. Chao, C.C. Liao, S.W. Fan, S.H. Wu, T.H. Hsieh, I.F. Sun, Y.L. Kuo and C.F. Hsieh. 2010. Lowland rainforests in southern Taiwan and Lanyu, at the northern border of Paleotropics and under the influence of monsoon wind. Plant Ecology **210(1)**: 1-17.

Chiou, C.R., Y.C. Liang, Y.J. Lai and M.Y. Huang. 2004. A study of delineation and application of the climatic zones in Taiwan. Journal of Taiwan Geographic Information Science **1(1)**: 41-62. [in Chinese with English summary]

Chiou, C.R., G.-Z. M. Song, J.H. Chien, C.F. Hsieh, J.C. Wang, M.Y. Chen, H.Y. Liu, C.L. Yeh, Y.J. Hisa and T.Y. Chen. 2010. Altitudinal distribution patterns of plant species in Taiwan are mainly determined by the northeast monsoon rather than the heat retention mechanism of Massenerhebung. Bot. Stud. **51**: 89-97.

Chiu, C.A. 2004. Regionalized mountain vegetation and predicted potential vegetation-The application of climate-vegetation classification scheme. Shei-Pa National Park Headquarters, Miaoli, Taiwan, ROC, 42pp. [in Chinese]

Chiu, C.A. and P.H. Lin. 2004. Spatial Interpolation of air temperature and precipitation from meteorological stations at Taiwan. Atmospheric Sciences **32(4)**: 329-350. [in Chinese with English summary]

Chiu, C.A., P.H. Lin and C.Y. Tsai. 2014. Spatio-temporal variation and monsoon effect on the temperature lapse rate of a subtropical island. Terr. Atmos. Ocean Sci. **25(2):** 203-217.

Daly, C., W.P. Gibson, G.H. Taylor, G.L. Johnson, and P.Pasteris. 2002. A knowledge-based approach to the statistical mapping of climate. Clim. Res. **22**:99-113.

Guan, B. T., H. W. Hsu, T. H. Wey and L. S. Tsao. 2009. Modeling monthly mean temperatures for the mountain regions of Taiwan by generalized additive models. Agr. Forest Meteorol. **149(2)**: 281-290.

Hannaway, D.B., C. Daly, W.X. Cao, W.H. Luo, Y.R. Wei, W.L. Zhang, A.G. Xu, C.A. Lu, X.Z. Shi and L.X. Li. 2005. Forage species suitability mapping for China using topographic, climatic and soils spatial data and quantitative plant tolerances. Agr. Sci. China **4(9)**: 660-667.

Harris, I., P.D. Jones, T.J. Osborn and D.H. Lister. 2014. Updated high-resolution grids of monthly climatic observations-the CRU TS 3.10 Dataset. Int. J. Climatol. **34(3)**: 623-642.

Hijmans, R.J., S.E. Cameron, J.L. Parra, P.G. Jones and A. Jarvis. 2005. Very high resolution interpolated climate surface for global land areas. Int. J. Climatol. **25(15)**: 1965-1978.

Hsu, H.H., C. Chou, Y.C. Wu, M.M. Lu, C.T. Chen and Y.M. Chen. 2011. Climate Change in Taiwan: Scientific Report 2011 (Summary). National Science Council, Taipei, Taiwan, ROC, 67pp.

Lenoir, J., J.C. Gegout, P.A. Marquet, P. de Ruffary and H. Brisse. 2008. A significant upward shift in plant species optimum elevation during the 20th century. Science **320(5884)**: 1768-1771.

Li, C.F., M. Chytry, D. Zeleny, M.Y. Chen, T.Y. Chen, C.R. Chiou, Y.J. Hsia, H.Y. Liu, S.Z. Yang, C.L. Yeh, J.C. Wang, C.F. Yu, Y.J. Lai, W.C. Chao and C.F. Hsieh. 2013. Classification of Taiwan forest vegetation. Appl. Veg. Sci. **16**: 698-719.

Lin, C. ., C.F. Li, D. Zeleny, M. Chytry, Y. Nakamura, M. Y. Chen, T.Y. Chen, Y.J. Hsia, C.F. Hsieh, H.Y. Liu, J.C. Wang, S.Z. Yang, C.L. Yeh and C.R. Chiou. 2012. Classification of the high-mountain coniferous forests in Taiwan. Foilia Geobot **47**: 373-401.

Lin, L.Y. 2011. Annual report on Taiwan Climate Change Projection and Information Platform (TCCIP) project. NSC98-2625-M-492-011. National Science Council, Taipei, Taiwan, ROC, 166 pp. [in Chinese with English summary]

Pepin, N. 2001. Lapse rate changes in northern England. Theoretical and Applied Climatology **68(1-2)**: 1-16.

Su, H.J. 1984a. Studies on the climate and vegetation types of the natural forests in Taiwan (I). Analysis of the variations in climatic factors. Quarterly Jounal of Chinese Forestry **17(3)**: 1-14.

Su, H.J. 1984b. Studies on the climate and vegetation types of the natural forests in Taiwan (II). Altitudinal vegetation zones in relation to temperature gradient. Quarterly Jounal of Chinese Forestry **17(4)**: 57-73.

Su, H.J. 1985. Studies on the climate and vegetation types of the natural forests in Taiwan (III). A scheme of geographical climatic regions. Quarterly Jounal of Chinese Forestry **18(3)**: 33-44.

Sun, I.F. 1993. The species composition and forest structure of a subtropical rain forest at southern Taiwan. PhD Thesis, University of California, Berkeley, USA.

Sun, I.F., C.F. Hsieh and S.P. Hubbell. 1998. The structure and species composition of a subtropical monsoon forest in southern Taiwan on a steep wind-stress gradient. In: Dallmeier, F. and J. A. Comiskey (eds) Forest Biodiversity Research, monitoring and modeling: conceptual background and old word case studies. Parthenon Publishing Co., Paris, France, pp 565-635.

Tang, C.Q. 2006. Forest vegetation as related to climate and soil conditions at varying altitudes on a humid subtropical mountain, Mount Emei, Sichuan, China. Ecological Research **21(2)**: 174-180.

Tang, C.Q. and M. Ohsawa. 1997. Zonal transition of evergreen, deciduous, and coniferous forests along the altitudinal gradient on a humid subtropical mountain, Mt. Emei, Sichuan, China. Plant Ecology **133**:63-78

Wang, T., A. Hamann, D. Spittlehouse and S.N. Aitken. 2006. Development of scale-free climate data for western Canada for use in resource management. Int. J. Climatol. **26(3)**: 283-397.

Wang T., A. Hamann, D. Spittlehouse and C. Carroll. 2016. Locally downscaled and spatially customizable climate data for historical and future periods for North America. PLoS One **11**(6): e0156720.

Wang, T., A. Hamann, D. Spittlehouse and T.Q. Murdock. 2012. ClimateWNA-high-resolution spatial climate data for Western North America. J. Appl. Meteorol. Climatol. **51(1)**: 16-29.

Wang, T., G. Wang, J.L. Innes, B. Seely and B. Chen. 2017. ClimateAP: an application for dynamic local downscaling of historical and future climate data in Asia Pacific. Frontiers of Agricultural Science and Engineering **4**(4): 448-458.

Weng, S.P. and C.T. Yang. 2012. The construction of monthly rainfall and temperature dataset with 1km gridded resolution over Taiwan area (1960-2009) and its application to climate projection in the near future (2015-2039). Atmospheric Sciences **40**(4): 349-369. [in Chinese with English summary]

Willmott, C.J. and K. Matsuura. 2009. Terrestrial Air Temperature and Precipitation: Monthly Climatologies (version 4.01). Global Air Temperature and Precipitation Archive.